



Improved cyclic stability of Mg_2Si by direct carbon coating as anode materials for lithium-ion batteries



Chengmao Xiao, Ning Du, Hui Zhang, Deren Yang*

State Key Lab of Silicon Materials and Department of Materials Science and Engineering, Cyrus Tang Center for Sensor Materials and Applications, Zhejiang University, Hangzhou 310027, People's Republic of China

ARTICLE INFO

Article history:

Received 9 July 2013

Received in revised form 14 October 2013

Accepted 15 October 2013

Available online 28 October 2013

Keywords:

Mg_2Si

Carbon layer

Lithium-ion batteries

Cyclic stability

ABSTRACT

High-crystalline Mg_2Si/C composites with uniform carbon layer were successfully synthesized by the decomposition of C_2H_2 gas onto the surface of pre-synthesized Mg_2Si . The Mg_2Si/C composites with a carbon content of 1.19% delivered a discharge capacity of 320 mA h g^{-1} after 100 cycles and a stable Coulombic efficiency over 95% after the first cycle, which is better than the bare Mg_2Si . The uniform carbon layer could enhance the electronic conductivity, buffer the volume change and reduce the pulverization during the charge/discharge process, which might be responsible for the enhanced cyclic performance. The results indicate that the chemical vapor deposition (CVD) of the carbon layer with low carbon content can distinctly enhance the cyclic stability of Mg_2Si , which can be extended to other anode materials.

© 2013 Elsevier B.V. All rights reserved.

1. Introduction

Nowadays, lithium-ion batteries (LIBs) are developed to high energy density and long cycle performance owing to the increasing demand for the energy consumption, especially from portable electronics and electric vehicles [1,2]. Recently, large effort has been devoted to explore new anode materials with high capacity such as silicon [3,4], tin or tin oxide [5,6], transitional metal oxides [7,8] and alloy compounds [9–11]. Among them, silicon-based alloy compounds, such as SiAl, SiMn, SiCu and SiMg attract much attention due to good cyclic performance compared to bare Si [12–19]. As a typical Si-based alloy compound, Mg_2Si has attracted much attention because of the following advantages: firstly, both Mg and Si are light-weight elements which is beneficial to achieve high mass energy; secondly, both Mg and Si can be inserted with lithium ions; thirdly, the specific capacity of Mg_2Si is much higher than that of commercial graphite [20–24]. However, Mg_2Si suffers large volume expansion during the intercalation and de-intercalation process, which leads to fast capacity fading.

Carbon coating has been widely used to improve the performance of the silicon and alloy-based anode materials [25–29] since it can enhance the electrical conductivity of active materials and tolerate the volume expansion during the intercalation/de-intercalation process [31–33]. In recent years, the synthesis of Mg_2Si/C as anode materials of LIBs has been investigated [20–24]. Usually, the ball-milling method was used for carbon coating, in which the

content of carbon was always very high. For example, Yan et al. synthesized Mg_2Si/C composites as anode materials of LIBs [12]. Through the optimization of the experimental conditions, the Mg_2Si/C delivered a reversible capacity of about 400 mA h g^{-1} with 40% carbon in the composite after 30 cycles. However, the carbon coating of Mg_2Si was not uniform and the carbon content was too high to achieve high energy density, which is unfavorable for commercial application.

In this work, we presented the synthesis of Mg_2Si/C composites via a CVD deposition of the carbon layer on the surface of pre-synthesized Mg_2Si particles. The experimental conditions were optimized and the electrochemical performance was studied. The results indicated that the CVD deposition of the carbon layer can improve the cyclic stability of the Mg_2Si anode with relatively low carbon content.

2. Experimental

Mg_2Si (purity, >95%) was synthesized via a home-built continuous preparing apparatus using Si (purity, >99%) and Mg (purity, >99%) powder as sources. Typically, Mg and Si powder with a molar ratio of 2:1 were added into a 100-ml grinding bowl. The ratio between the raw materials and the grinding balls is 1:6. Then, milling was performed at a rotating rate of 500 rpm for 6 h under Ar atmosphere. After milling, the mixture was annealed at $600 \text{ }^\circ\text{C}$ for 2 h under Ar atmosphere. For Mg_2Si/C composite, 0.3 g Mg_2Si was loaded in a furnace with a constant C_2H_2/Ar mix gas (1:10, volume ratio) flowing. The furnace was then heated to different reacting temperatures and preserved for different reacting time. To optimize the experimental conditions, 6 experiments with different reacting time and temperatures have been done, as shown in Table 1.

An X-ray diffractometer (PANalytical) was used to characterize the phases of the products. The morphology of the products was identified by scanning electron microscopy (SEM, Hitachi S4800) and transmission electron microscopy (TEM,

* Corresponding author. Tel.: +86 571 87953190; fax: +86 571 87952322.

E-mail address: mseyang@zju.edu.cn (D. Yang).

Table 1
Experiment conditions with different reacting time and temperatures.

Group	a	b	c	d	e	f
Temperature (°C)	450	500	550	450	450	450
Reaction time	1 h	1 h	1 h	1 h	3 h	6 h

F200). The carbon contents were measured with an Element analyzer (EA1119). For electrochemical test, a two-electrode cells with lithium metal as the counter has been carried out. The electrode was prepared as follow: Mg_2Si/C , acetylene black and polyvinylidene fluoride with a mass ratio of 80:10:10 were first dissolving in N-methyl-2-pyrrolidone (NMP) to get uniform slurry. Then, the mixture was pasted on the copper foils. After dried at 120 °C under vacuum for 12 h, the copper foils were then pressed with a pressure of 20 MPa. The cells were assembled in an argon-filled glove box. The electrolytes were 1 M $LiPF_6$ dissolved in a mixture of ethylene carbonate (EC) and diethyl carbonate (DEC) with the volume ratio of EC/DEC = 1:1 (volume ratio). The cyclic performance was evaluated on a LAND CT2001A system between 0.01 and 3.0 V with a current density of 100 mA g^{-1} . Cyclic voltammetry (CV) were recorded at a scan rate of 0.1 $mV s^{-1}$.

3. Results and discussion

3.1. XRD characterization of the Mg_2Si/C

Fig. 1 shows the XRD patterns of the as-synthesized Mg_2Si and Mg_2Si/C . Compared to the as-synthesized Mg_2Si (the black line), the peaks of Mg_2Si/C show no change after the coating of carbon layer at 450 °C due to the amorphous nature of the carbon layer. Fig. 2a shows the XRD patterns of Mg_2Si/C at different coating temperatures (450, 500 and 550 °C) for 1 h. It can be seen that other peaks related to Si and MgO emerge and their intensity increases along with the increasing reacting temperatures. The intensity of the impurity peaks in the XRD patterns also increases along with the reacting time (Fig. 2b). The XRD results indicate that Mg_2Si is unstable at high temperature and can be decomposed to Si and Mg, while the metal Mg is easily oxidized by the residual oxygen in the furnace. Therefore, the appropriate reacting temperature and time for carbon coating is 450 °C and 1 h, respectively.

3.2. Morphology of the Mg_2Si/C

The morphology of the as-synthesized Mg_2Si is shown in Fig. 3a. As can be seen, the as-synthesized Mg_2Si are inhomogeneous particles with a size of several micrometers, which accumulate and attach to each other to form large particles. After the coating of the carbon layer, the morphology (Fig. 3b) is almost the same as the bare one, while the surface turns rough. The TEM image (Fig. 3c) of the Mg_2Si/C composite shows the irregular particles with the

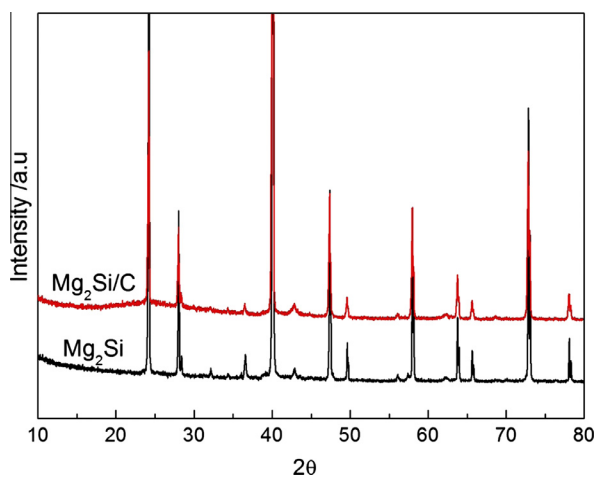


Fig. 1. XRD patterns of the as-synthesized Mg_2Si and Mg_2Si/C composite at 450 °C.

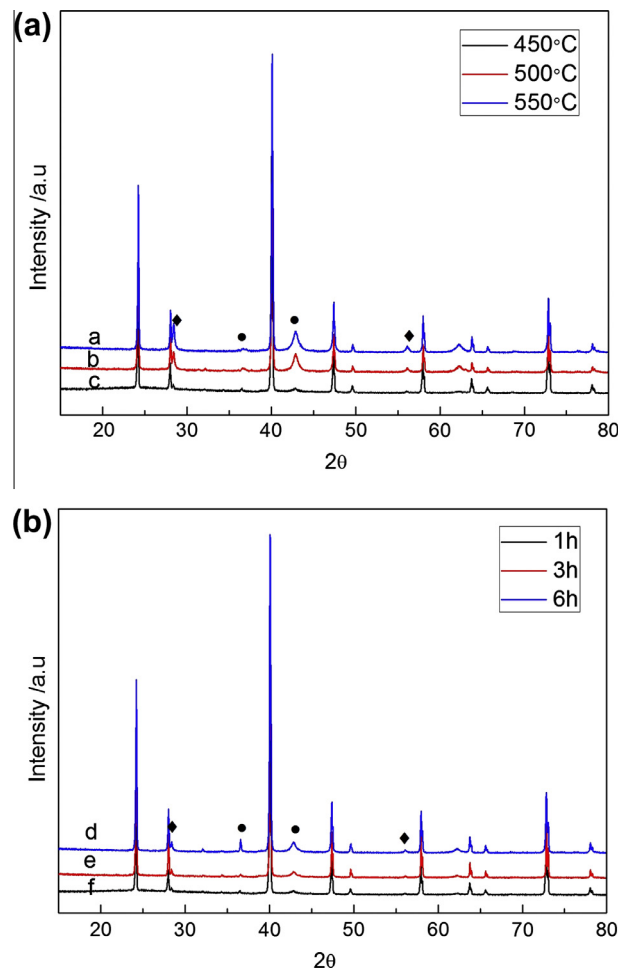


Fig. 2. XRD patterns of the products with different conditions: (a) at the reaction temperatures of 450, 500, and 550 °C coating for 1 h, respectively; (b) and at 450 °C for the reaction time of 1, 3, 6 h, respectively (♦ is the peak of Si, ● represents the MgO, the others are the peaks of Mg_2Si).

size of several hundred nanometers, which may be peeled off from the large Mg_2Si/C particles during the preparation of TEM samples. Fig. 3d shows the high-resolution TEM (HRTEM) image of an individual Mg_2Si/C particle. It can be seen that a thin carbon layer of 2–3 nm has been deposited onto the surface of Mg_2Si , indicating that the carbon content in the composite is very low. The low carbon content can also be identified by the element analysis characterization, indicating that the content of the carbon is 1.19%. It should be mentioned that the low carbon content is beneficial to high volumetric energy density since the density of the carbon is usually lower than the active materials.

3.3. Electrochemical performance of Mg_2Si/C

The Mg_2Si/C composite was tested as anode materials of LIBs. Fig. 4 shows the first three cyclic voltammogram (CV) curves of Mg_2Si/C between 0.01 and 1.5 V at a scan rate of 0.1 $mV s^{-1}$. It can be seen that two weak peaks locate at 0.67 and 0.1 V in the first lithium insertion process, respectively. The peak at 0.1 V is due to the lithium insertion into Mg_2Si to form Li_2MgSi ternary phase [19,22]. It should be mentioned that there is only one peak at 0.1 V due to the carbon coating, which is consistent with the previous report [22]. The peak at 0.67 V is attributed to the formation of the SEI film [30]. For the anodic process, there are three anodic peaks at 0.2, 0.3 and 0.7 V, which are the typical anodic peaks for carbon-coated Mg_2Si . After the first cycle, the anodic

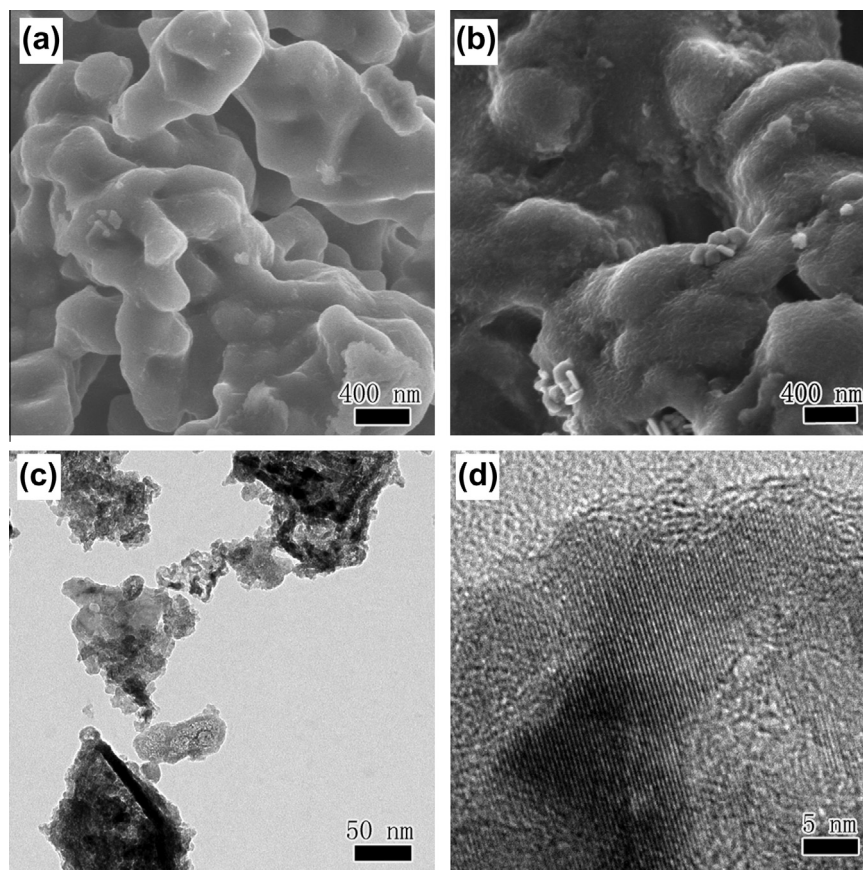


Fig. 3. SEM images of the as-synthesized Mg_2Si (a) and $\text{Mg}_2\text{Si}/\text{C}$ (b); And low-(c) and high-magnified (d) TEM images of $\text{Mg}_2\text{Si}/\text{C}$.

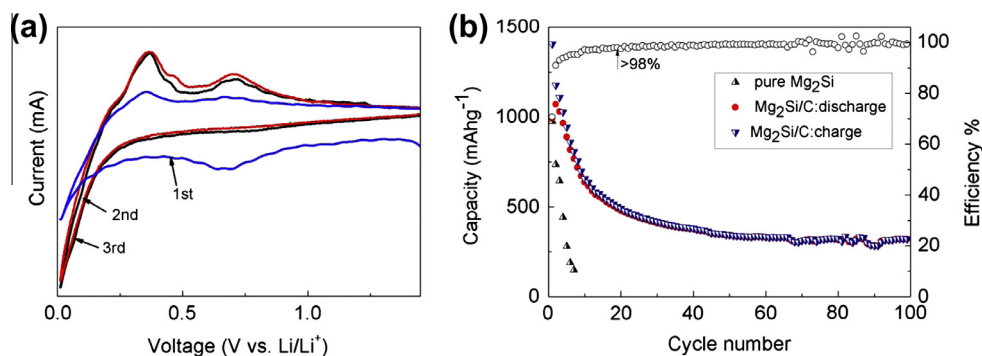


Fig. 4. (a) The first three CV curves of $\text{Mg}_2\text{Si}/\text{C}$ composite in the potential range of 0.0–1.5 V at a scan rate of 0.1 mV s^{-1} ; (b) long cyclic performance of the pure Mg_2Si and the carbon coating sample, where the testing current was 100 mA g^{-1} in the potential range of 0.01–3.0 V.

peaks become stable and locate at 0.2–0.3 and 0.6–0.7 V, which may be attributed to carbon layer. The carbon layer can help to establish the stable SEI film during the alloying process. The cyclic performance of the $\text{Mg}_2\text{Si}/\text{C}$ anode in the CR2021 cells is tested at a current of 100 mA g^{-1} in the potential between 0.01 and 3 V. For bare Mg_2Si , the initial discharge capacity is $988.7 \text{ mA h g}^{-1}$ and it decreases to 94.7 mA h g^{-1} after 7 cycles. In comparison, the $\text{Mg}_2\text{Si}/\text{C}$ composite shows the first discharge and charge capacity of 1405.3 and $993.7 \text{ mA h g}^{-1}$, respectively, indicating the initial Coulombic efficiency of 70.7%. The capacity loss in the first cycle is mainly due to the formation of SEI film. After the first cycle, the capacity of the $\text{Mg}_2\text{Si}/\text{C}$ composite begins to decay which is due to the large volume change during the charge/discharge process. However, the capacity fades slowly

after 10 cycles, and a high Coulombic efficiency over 98% is obtained. Even after 100 cycles, a constant capacity over 320 mA h g^{-1} can be achieved. The great improvement of the cyclic stability may be attributed to the thin carbon layer, which could enhance the electronic conductivity, buffer volume change, and stabilize the SEI film during the charge/discharge process. The carbon layer can tolerate the volume expansion to some extent due to its good elasticity, which has also been proposed by previous papers [31–33]. It can be seen from Fig. 5 that the carbon layer can accommodate the strain induced by the volume change during the alloying process due to its elasticity. Furthermore, the carbon layer can help to form a stable SEI film that can prevent the active materials to directly contact with the electrolyte, which may also facilitate the cyclic stability.

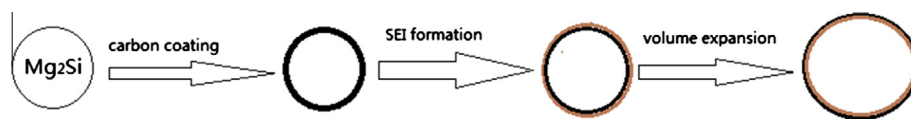


Fig. 5. Schematic illustration of the $\text{Mg}_2\text{Si}/\text{C}$ composite during the alloyed process.

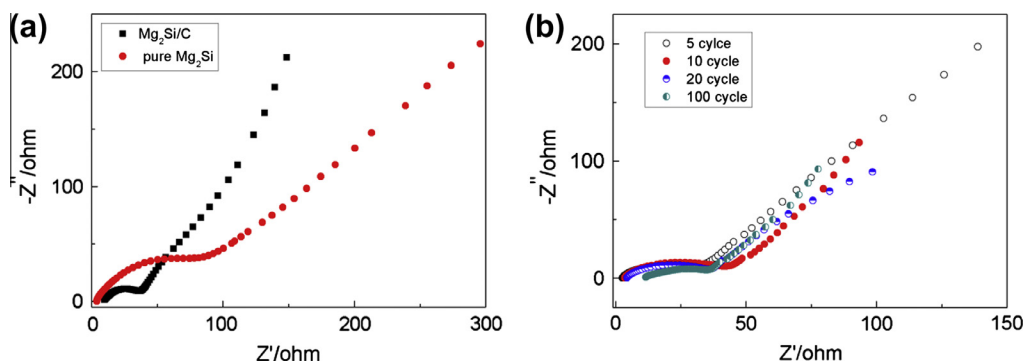


Fig. 6. The ac impedance spectra of pure Mg_2Si and $\text{Mg}_2\text{Si}/\text{C}$ composites: (a) before cycling; (b) different cyclic performance of the $\text{Mg}_2\text{Si}/\text{C}$ composite.

In order to understand the improvement of the electronic conductivity induced by the carbon layer, EIS experiments of the bare Mg_2Si and $\text{Mg}_2\text{Si}/\text{C}$ composite have been carried out before and after cycling (Fig. 6). The high frequency semicircle is attributed to the SEI film and contact resistance. The semicircle in the medium frequency region is assigned to the charge transfer resistance R_{ct} , and its value is approximately equal to the diameter of the semicircle [34,35]. The inclined line at low frequency corresponds to the diffusion of lithium ions in the electrodes, which can be identified by Z_w . Z_w is the Warburg impedance, representing the diffusion resistance in the electrode bulk [32,3]. As observed, the charge transfer resistance of the bare Mg_2Si is 126.9 Ω . In contrast, the charge transfer resistance of the $\text{Mg}_2\text{Si}/\text{C}$ composite is only 39.2 Ω , which is much lower than that of the bare Mg_2Si (Fig. 6a). The decreased value of the charge transfer resistance indicates the enhanced conductivity of $\text{Mg}_2\text{Si}/\text{C}$. Furthermore, the EIS plots of different cycling number are also presented, as showed in Fig. 6b. It can be seen that the diameters of the $\text{Mg}_2\text{Si}/\text{C}$ are all slightly increasing in the following cycles in addition to the first cycle. However, the diameters after the 10th cycling number seem almost no difference, indicating that the $\text{Mg}_2\text{Si}/\text{C}$ electrode has stable reactive interface with the electrolyte (Fig. 6b). The 10th semicircle diameter is slightly bigger than other cycles, which may be owing to the fluctuation of the interface resistance R_{int} at the initial cycles. The surface layer may be destroyed by the de-intercalation of lithium-ion. After the initial several cycles, a stable SEI film could be generated by the assistance of the carbon layer. The results of the EIS impedance correlate well with the cyclic performance and the analysis of the carbon layer.

4. Conclusions

In summary, $\text{Mg}_2\text{Si}/\text{C}$ composite was synthesized by decomposition of C_2H_2 onto the pre-synthesized Mg_2Si . The thickness of the carbon layer could be adjusted by the reacting temperatures and time. When used as anode materials of LIBs, the $\text{Mg}_2\text{Si}/\text{C}$ composite shows significantly improvement on cyclic performance compared to bare Mg_2Si . The great improvement of the cyclic stability may be attributed to the thin carbon layer, which could enhance the electronic conductivity, buffer volume change and reduce pulverization during the charge/discharge process.

Acknowledgments

The authors would like to appreciate the financial support from NSFC (No. 51002133), 973 Project (No. 2013BC632102), the 863 Project (No. 2011AA050517) and the Fundamental Research Funds for the Central Universities.

References

- [1] J.M. Tarascon, M. Armand, *Nature* 414 (2001) 359–404.
- [2] U. Kasavajjula, C. Wang, A.J. Appleby, *J. Power Sources* 163 (2007) 1003–1039.
- [3] F. Wang, S. Zhu, M. Li, X. Lou, K. Hui, S. Xu, P. Yang, L. Wang, Y. Chen, P. Chu, *J. Alloys Comp.* 563 (2013) 186–191.
- [4] Y. He, B. Yang, K. Kun, C. Brown, R. Ramasamy, H. Wang, C. Lundgren, Y. Zhao, *J. Mater. Chem.* 22 (2012) 8294–8303.
- [5] X. Wang, X. Cao, L. Bourgeois, H. Guan, S. Chen, Y. Zhong, D.M. Tang, H. Li, T. Zhai, L. Li, Y. Bando, D. Golberg, *Adv. Funct. Mater.* 22 (2012) 2682–2690.
- [6] B. Zhang, C. Wang, Q. Ru, S. Hu, D. Sun, X. Song, J. Li, *J. Alloys Comp.* 581 (2013) 1–5.
- [7] W. Mei, J. Huang, L. Zhu, Z. Ye, Y. Mai, J. Tu, *J. Mater. Chem.* 93 (2012) 15–22.
- [8] L. Hu, Y. Sun, F. Zhang, Q. Chen, *J. Alloys Comp.* 576 (2013) 86–92.
- [9] R.M. Gnanamuthu, Y.N. Jo, C.W. Lee, *J. Alloys Comp.* 02 (2013) 146.
- [10] J. Yu, N. Du, J. Wang, H. Zhang, D. Yang, *J. Alloys Comp.* 577 (2013) 564–568.
- [11] R. Jin, Z. Liu, L. Yang, J. Liu, Y. Xu, G. Li, *J. Alloys Comp.* 579 (2013) 209–217.
- [12] Y.N. Li, B. Wang, J. Yang, X. Yuan, Z. Ma, *J. Power Sources* 153 (2006) 371–374.
- [13] P. Zuo, G. Yin, Y. Tong, *Solid State Lett.* 177 (2006) 3297–3301.
- [14] H.J. Ahn, Y.S. Kim, K.W. Park, T.Y. Seong, *Chem. Commun.* 1 (2005) 43–45.
- [15] T.D. Hatchard, M.N. Obrovac, J.R. Dahn, *J. Electrochem. Soc.* 153 (2006) A282–A287.
- [16] T.D. Hatchard, J.R. Dahn, *J. Electrochem. Soc.* 152 (2006) A1445–A1451.
- [17] J. Wolfenstijn, *J. Power Sources* 124 (2003) 241–245.
- [18] Y.M. Kang, M.S. Park, J.Y. Lee, H.K. Liu, *Carbon* 45 (2007) 1928–1933.
- [19] S. Zhou, D. Wang, *ACS Nano* 11 (2010) 7014–7020.
- [20] G.A. Roberts, E.J. Cairns, J.A. Reimer, *J. Power Sources* 110 (2002) 424–429.
- [21] S.W. Song, K.A. Strebler, X. Song, E.J. Cairns, *J. Power Sources* 119 (2003) 110–112.
- [22] J.M. Yan, H.Z. Huang, J. Zhang, Y. Yang, *J. Power Sources* 175 (2008) 547–552.
- [23] Y. Liu, Y. He, R. Ma, M. Gao, H. Pan, *Electrochem. Commun.* 25 (2012) 15–18.
- [24] T. Moriga, K. Watanabe, D. Tsuji, S. Massaki, I. Nakabayashi, *J. Solid State Chem.* 153 (2000) 386–390.
- [25] M. Wang, L. Fan, M. Huang, J. Li, X. Qu, *J. Power Sources* 219 (2012) 29–35.
- [26] W. Zhou, S. Upreti, M. Whittingham, *Electrochem. Commun.* 13 (2011) 1102–1104.
- [27] Y. Qi, N. Du, H. Zhang, P. Wu, D. Yang, *J. Power Sources* 196 (2011) 10234–10239.
- [28] J. Chong, S. Xun, X. Song, P. Ridgway, G. Liu, V. Battaglia, *J. Power Sources* 200 (2012) 67–76.

- [29] K.H. Seng, M.H. Park, Z.P. Guo, H.K. Liu, J. Cho, *Angew. Chem. Int. Ed.* 51 (2012) 5657–5661.
- [30] X. Yang, Z. Wen, X. Xu, B. Lin, S. Huang, *J. Power Sources* 164 (2007) 880–884.
- [31] S. Yang, Q. Pan, J. Liu, *Electrochem. Commun.* 12 (2010) 479–482.
- [32] T. Kim, Y.H. Mo, K.S. Nahm, S.M. Oh, *J. Power Sources* 162 (2006) 1275–1281.
- [33] V.G. Khomenko, V.Z. Barsukov, J.E. Doninger, I.V. Barsukov, *J. Power Sources* 165 (2007) 598–608.
- [34] A.J. Bard, L.R. Faulkner, *Electrochemical Methods*, second ed., John Wiley & Sons, New York, 2001. p. 231.
- [35] A.Y. Shenouda, Hua K. Liu, *J. Electrochem. Soc.* 157 (2010) A1183–A1187.